Occurrence and Spatial Extent of HABs on the West Florida Shelf 2002–Present

Ruhul Amin, Bradley Penta, and Sergio deRada

***Abstract*—Harmful algal blooms (HABs) can lead to severe economic and ecological impacts in coastal areas and can threaten marine life and human health. About three quarters of these toxic blooms are caused by dinoflagellate species. One dinoflagellate species, i.e., *Karenia brevis*, blooms nearly every year in the Gulf of Mexico, particularly on the West Florida Shelf (WFS), where these blooms cause millions of dollars in socioeconomic damage. In this letter, we use the red band difference (RBD) bloom detection technique for detection of low backscattering phytoplankton blooms, such as *K. brevis*, and conduct time-series analyses of the spatial extent of these blooms using Moderate Resolution Imaging Spectroradiometer (MODIS) monthly mean data spanning July 2002 (sensor inception) to September 2014. The time-series results show that the RBD successfully detects the documented HABs in the region, illustrating the seasonal and interannual variability, including the extensive blooms of 2005 and 2014.**

***Index Terms*—Harmful algal blooms (HABs), *karenia brevis*, low backscattering blooms (LBBs), phytoplankton, red band difference (RBD), remote sensing.**

I. Introduction

HARMFUL algal blooms (HABs) have been known to occur throughout human history, and in recent years, HABs have become a major environmental problem affecting coastal areas globally. The nature of the problem has expanded both in extent and public perception. Human activities and population growth have contributed to increases in various noxious algal species in coastal regions worldwide [1], [2]. Eutrophication in estuaries and coastal waters is believed to be a major factor causing HABs [3], [4]. Whereas HABs can be composed of several classes of microalgae, including diatoms, dinoflagellates, raphidophytes, cyanobacteria, prymnesiophytes, pelagophytes, and silicoflagellates [5], approximately 75% of all HAB species are dinoflagellates [6], [7]. Marine HABs generally occur in warm regions or seasons and in places with elevated nutrient levels such as coastal waters influenced by agricultural activity from inland regions [8]. The unique ecophysiology of these organisms favors their increasingly successful exploitation of coastal waters and global bloom expansion [9].

Manuscript received June 10, 2015; accepted June 15, 2015. Date of publication July 16, 2015; date of current version August 7, 2015. This work was supported in part by the Center for the Advancement of Science in Space through NASA Cooperative Agreement NNH11CD70A, by the NRL project "Modeling Dynamic Bio-Optical Layers In Coastal Systems (DYaBOLIC)" under Program Element 61153N, and by a grant from BP/The Gulf of Mexico Research Initiative to the DEEP-C Consortium (#SA 12-12, GoMRI-008).

R. Amin is with BioOptoSense LLC, New Orleans, LA 70115 USA (e-mail: biooptosense@gmail.com).

B. Penta and S. deRada are with the Naval Research Laboratory, Stennis Space Center, Hancock County, MS 39529 USA.

Color versions of one or more of the figures in this paper are available online at http://ieeexplore.ieee.org.

Digital Object Identifier 10.1109/LGRS.2015.2448453

According to the Florida Conservation Commission (http://www.floridaconservation.org/), more than 40 species of toxic microalgae live in the Gulf of Mexico, but the most common bloom-forming species is the toxic dinoflagellate *Karenia brevis* (syn. *Gymnodinium breve* and *Ptychodiscus brevis*). Although *K. brevis* blooms have been reported throughout the Gulf of Mexico, they are most frequent along the West Florida Shelf (WFS), where they occur nearly every year, usually between late summer and early spring. *K. brevis* blooms produce brevetoxin that causes neurotoxic shellfish poisoning, leading to death in fish, birds, and marine mammals [10]. Brevetoxin can irritate human eyes and respiratory systems once it becomes aerosolized in sea spray [11], [12]. Although no human fatalities have been directly attributed to brevetoxin, toxin levels potentially fatal to humans can be reached during *K. brevis* blooms [5], [13].

Optical remote sensing (ocean color) techniques are well suited to study species such as vertically migrating dinoflagellates (including *K. brevis*) that aggregate at the surface for photosynthesis during the day. Their dense aggregations produce strong bio-optical signals that can be detected by spaceborne and airborne optical sensors. There has been considerable interest in using satellite measurements to study blooms since these measurements can provide us with high spatial and temporal resolution, early bloom detection, and guidance for *in situ* sampling and can reveal important spatiotemporal evolution of blooms by either growth or advection by physical processes. In addition, assimilation of satellite chlorophyll imagery into coupled biophysical models has recently been achieved [14], and development of specific satellite-derived dinoflagellate products will lead to their assimilation into ecological models and improved forecasting capability.

Many techniques have been developed to detect algal blooms in the Gulf of Mexico. Stumpf *et al.* [15] proposed the use of the magnitude of the difference between satellite chlorophyll concentration estimates and a background mean of the previous 0.5–2.5 months' chlorophyll estimates as an index for detecting bloom areas. This method is now used operationally at NOAA NESDIS CoastWatch to alert for possible blooms. Cannizzaro *et al.* [16] proposed another technique based on *in situ* data that uses the backscattering/chlorophyll ratio to discriminate between *K. brevis* and other blooms. They determined that *K. brevis* has lower backscatter characteristics than blooms of diatoms and other dinoflagellate species. Both of these methods are based on using the blue–green region of the spectrum. However, blue–green reflectance ratio algorithms [17]–[19] have been found to perform poorly in coastal waters due to increased absorption of chromophoric dissolved organic matter (CDOM), increased particle scattering, inaccurate atmospheric corrections, and reflectance from shallow bottoms [20]–[23].

1545-598X © 2015 IEEE. Translations and content mining are permitted for academic research only. Personal use is also permitted, but republication/redistribution requires IEEE permission. See http://www.ieee.org/publications_standards/publications/rights/index.html for more information.

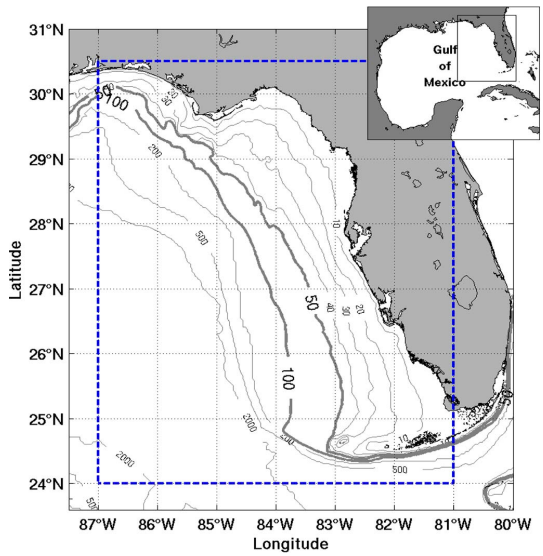

Fig. 1. WFS. Study area is highlighted in blue. Gray contours are bathymetric isobaths.

Thus, the red spectral region is particularly attractive for our use since it is less contaminated by CDOM and bottom reflectance and is less susceptible to atmospheric correction inaccuracies than the blue–green region. Consequently, uncertainties in bloom detection algorithms are reduced when the red spectral region is used instead of the blue–green region. Moderate Resolution Imaging Spectroradiometer (MODIS) red bands (677 and 678 nm) were designed with high signal-to-noise ratios for retrievals of fluorescence and, hence, chlorophyll [24]–[27]. The fluorescence line height (FLH) algorithm [24]–[26] uses these bands to compute a proxy for chlorophyll. However, in highly scattering waters, typical of coastal areas, the fluorescence component represents a small portion of the total reflectance signal, and the FLH erroneously extracts a combined elastic scattering and fluorescence signal rather than the much smaller fluorescence signal [28]–[30], resulting in false positives. As a refinement to the FLH algorithm, the red band difference (RBD) technique [31] was developed for detection of low backscattering blooms (LBBs), which include *K. brevis* and other athecate dinoflagellate species. When low backscattering conditions exist, the red spectral region becomes chlorophyll fluorescence dominated, and the RBD takes advantage of this signal to detect blooms. Consequently, in highly scattering waters, the RBD does not give false positives. Since the RBD is insensitive to atmospheric correction and less sensitive to CDOM absorption and bottom reflectance, it can more accurately distinguish blooms from other bloom-like features, such as CDOM and sediment plumes, making it an effective tool for LBB detection.

II. Data and Methods

A. Satellite Data

We used calibrated Level 1B MODIS-Aqua data (http://ladsweb.nascom.nasa.gov/) and processed them using the Naval Research Laboratory's (NRL's) Automated Processing System (APS) [32]. For our study area (see Fig. 1), we constructed 1-km resolution monthly composites (i.e., weighted means of cloud-free pixels) of chlorophyll via the OC3 [18] algorithm and of LBB via the RBD [31] algorithm.

B. RBD Technique

The RBD technique, described in detail in [31], was developed for relatively low backscattering blooms such as those of *K. brevis*. In summary, this technique takes advantage of the chlorophyll fluorescence signal (emission centered on 685 nm) as an indicator of the bloom. Since there is nothing else in the water that fluoresces in the red region, the RBD easily distinguishes bloom regions from false bloom-like features such as CDOM plumes, sediment plumes, and bottom reflectance. This results in accurate bloom detection and precise bloom delineation. The RBD algorithm is defined as follows:

$$\mathrm{RBD} = \mathrm{nLw}(\lambda_2) - \mathrm{nLw}(\lambda_1) \tag{1}$$

where $\mathrm{nLw}(\lambda)$ is normalized water-leaving radiance, which is defined as the upwelling radiance just above the sea surface, in the absence of an atmosphere and with sun directly overhead. λ_1 represents MODIS band 13 (667 nm), and λ_2 represents MODIS band 14 (678 nm). The RBD technique was based on the principle that photosynthetic organisms absorb strongly around 675 nm, which causes $\mathrm{nLw}(\lambda)$ to have a trough around this band (see [31, Fig. 1]). Due to the contribution of chlorophyll fluorescence emission centered on 685 nm and the relatively lower backscattering efficiency of LBB species (such as *K. brevis*) [16], this trough is shifted toward shorter wavelengths around 667 nm, or below, depending on the concentrations of chlorophyll and the quantum yield of chlorophyll fluorescence [31], [33], [34]. Therefore, the signal around λ_2, which falls in the shoulder of the red–near-infrared(NIR) water-leaving radiance peak, has higher values than the signal around λ_1 due to the chlorophyll fluorescence contribution. Furthermore, a threshold is applied to discriminate blooms from the background signal. For *K. brevis* bloom detection, the value for this threshold was determined by Amin *et al.* [31] ($\mathrm{RBD} > 0.15$ W/m^2/μm/sr). Using satellite data (MODIS-Aqua from mid-August 2002 to December 2011) matched with *in situ K. brevis* cell count data from the Florida Fish and Wildlife Conservation Commission's Fish and Wildlife Research Institute (FWC-FWRI), Ramos [35] reevaluated the RBD threshold and concluded that the value from [31] is the appropriate threshold for *K. brevis* bloom detection. The RBD technique can also be used to quantify the blooms in terms of chlorophyll. Wernand *et al.*, [36] used a similar band difference approach to estimate high concentration of chlorophyll in the Western Wadden Sea and the North Sea using *in situ* data.

III. Results and Discussion

Bloom detection from ocean color measurements is usually hampered by uncertainties over optically complex coastal waters. These uncertainties arise from imperfect atmospheric correction, imperfect ocean color product retrieval algorithms, and interference from other bloom-like features such as CDOM and sediment plumes. Some of these uncertainties are reduced with red–NIR algorithms such as the RBD and the FLH. While both algorithms use a portion of the chlorophyll fluorescence signal to detect blooms [31], [37], FLH breaks down in highly

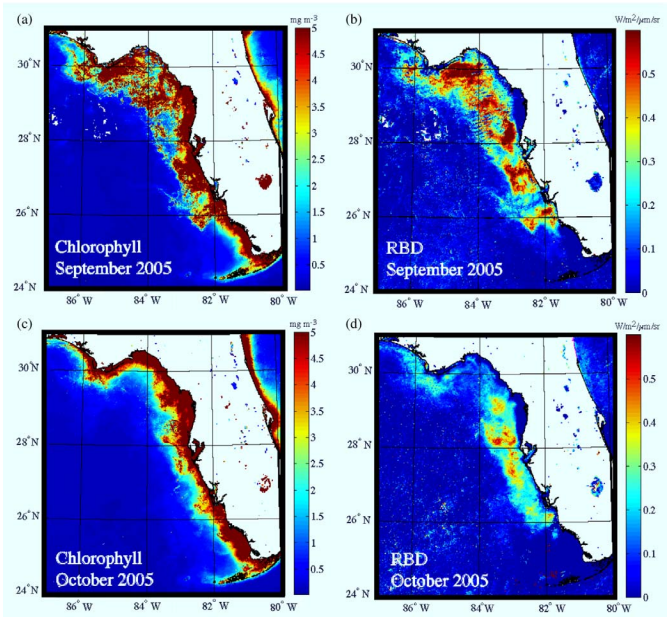

Fig. 2. MODIS monthly composite images. (a) September 2005 chlorophyll image. (b) Corresponding RBD image. (c) October 2005 chlorophyll image. (d) Corresponding RBD image.

scattering waters, where high red peak values are primarily due to contributions from elastic scattering modulated by chlorophyll absorption rather than fluorescence, thus falsely indicating possible blooms [28]–[30]. In contrast, the RBD technique does not give false-positive values in highly scattering waters [31]–[33], resulting in more precise bloom detection.

In coastal waters, the standard NIR atmospheric correction [38] often fails due to high turbidity, contributing significantly higher radiances in the NIR bands. Consequently, the water-leaving radiance at NIR can no longer be considered negligible for atmospheric correction in extreme blooms [39], [40]. Thus, negative readings may result in the blue–green bands due to the overcorrection of the atmosphere [41]. Even short-wave IR [42] atmospheric corrections have been found to occasionally give negative radiances in HAB regions, an indication of the limitations of atmospheric correction algorithms. These errors, larger in shorter wavelengths [33], [40], cause inaccurate values from retrievals using blue–green band ratio algorithms (e.g., OC4). Since RBD uses band differences of two near spectral bands over which the atmospheric impact is small, and more importantly, uses the difference rather than the ratio of the bands, it is insensitive to atmospheric correction [31], [33].

In addition to atmospheric correction uncertainties, CDOM absorption also causes significant uncertainties in chlorophyll retrieval from reflectance spectra in coastal waters [43]. Fig. 2 shows a qualitative comparison of monthly composite chlorophyll from September 2005 [see Fig. 2(a)], the corresponding RBD image [see Fig. 2(b)], the chlorophyll image from October 2005 [see Fig. 2(c)], and the corresponding RBD image [see Fig. 2(d)]. Although chlorophyll images sometimes show features in bloom regions, these numbers are usually not accurate due to the aforementioned uncertainties. Clearly seen in both chlorophyll images [see Fig. 2(a) and (c)], bloom-like features (warm colors) exist throughout the Florida coast due to the uncertainties associated with the blue–green bands. However, these features are not present in the RBD images [see Fig. 2(b) and (d)], demonstrating the efficacy of the RBD algorithm to isolate LBBs.

In 2005, Florida experienced the most significant HAB event in the MODIS record, covering an area of approximately 67 500 km^2 [44]. This event caused hypoxic zones off west-central Florida, and benthic communities, fish, turtles, birds, manatees and other marine mammals suffered extensive mortalities. With the standard RBD threshold, our estimate shows that the bloom area was about 60 000 km^2 for the September 2005 monthly composite image shown in Fig. 2(b). In the studied region, blooms are typically detected using the chlorophyll anomaly method [15] or the FLH [37]. However, unlike these methods, the RBD gives much more precise bloom location and extent due to its relative insensitivity to atmospheric correction, CDOM, and bottom reflectance. Thus, as expected, the RBD estimated area is smaller than the area documented in Hu *et al.* [44].

Two additional noise sources may result in overestimation of the LBB area by the RBD technique. Together, these noise sources appear as "salt and pepper" noise on RBD images [e.g., see Fig. 2(b) and (d)]. Clouds constitute one of the noise sources—from cloud-edge pixels and undetected (therefore, not masked) thin clouds. Since clouds are much brighter than water, photons reflected from the clouds are scattered by the atmosphere, brightening the neighboring water pixels (the adjacency effect [45]). The second source is due to the variation in the response among the red band detectors on the MODIS instrument. These variations are visible as striping at the end of each scan line on individual MODIS images. Application of the RBD threshold excludes some of these contaminated pixels; however, while raising the RBD threshold would reduce the "salt and pepper" noise, it would also remove real blooms with low concentrations. Removal of the noise sources would allow a more precise bloom area estimation with the RBD technique. Therefore, we are currently studying other approaches to reduce the effects of this noise and improve the accuracy of RBD spatial estimation. Since *K. brevis* blooms often extend hundreds of square kilometers, using the blob detection approach, as in our previous studies of clouds and shadows [46], [47], may improve LBB spatial extent estimation on the WFS. Fully resolving the remaining noise is ongoing research and outside the scope of this letter.

Fig. 3 shows the monthly mean bloom extent (in km^2) from RBD for the entire MODIS Aqua record (July 2002 to September 2014). *K. brevis* blooms occur almost every year between August and March and occasionally at other times [48]. This trend is clearly seen in the time-series plot in Fig. 3, where the striking event of 2005 and the more recent event (July–September 2014) are particularly evident. Since the 2005 bloom was exceptionally large relative to the rest of the years, it was excluded from the mean and standard deviation calculations (4892 and 4317 km^2, respectively). All of the data points above the lower standard deviation line (mean—STD) in Fig. 3 should represent blooms, but since the data have been filtered using the RBD threshold, there appear to be blooms nearly every month even during nonbloom seasons. This variability is due to the unfiltered "salt and pepper" noise and also due to blooms of other LBB species since the RBD is not *K. brevis* specific. Notwithstanding the "salt and pepper" noise, the RBD estimates a more precise bloom area than the chlorophyll anomaly or the FLH algorithms [31] when compared with the reported

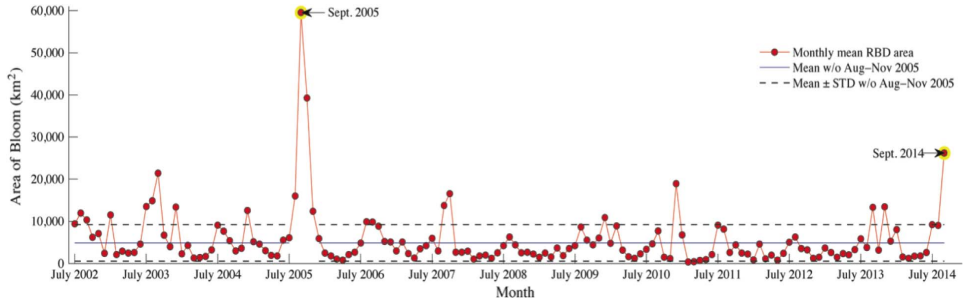

Fig. 3. Time series of LBBs (likely dominated by K. brevis) spatial extent estimated from MODIS monthly composite data for the study region.

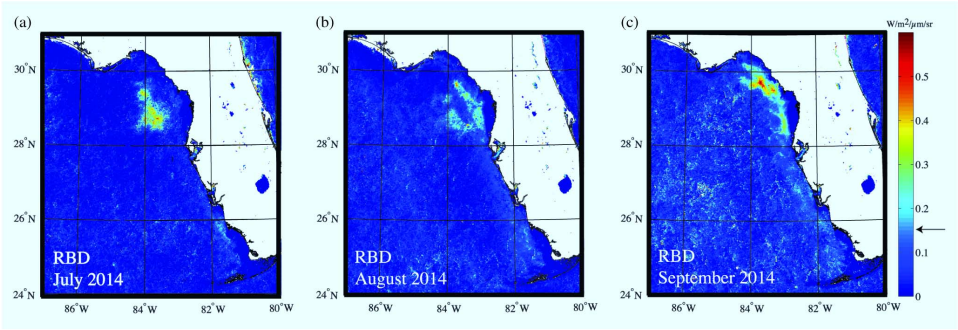

Fig. 4. Progression of the LBBs on the WFS using the RBD technique. (a) July 2014. (b) August 2014. (c) September 2014. The arrow on the colorbar indicates the RBD threshold.

bloom area [44]. Since nonbloom signals resemble "salt and pepper" noise, true bloom regions can be identified by an observer easily in the RBD images. Fig. 4 illustrates the coastward progression of the 2014 *K. brevis* bloom with RBD imagery from July to September [see Fig. 4(a)–(c)]. Bright "salt and pepper" like pixels can be observed in the figure, however, the bloom is a large, easily distinguished feature distinct from the "salt and pepper" noise.

IV. Conclusion

This letter complements previous research in bloom detection and shows further evidence that the RBD technique is indeed an effective detection tool for LBBs such as *K. brevis*. Substantiated by documented blooms [15], [16], [31], [37], applying the RBD technique to MODIS monthly composite data spanning the entire mission (July 2002–Septemper 2014) elucidates the seasonal and interannual dynamics of LBBs on the WFS. This letter also demonstrates the value of including the chlorophyll fluorescence channel in future satellite sensors such as those being planned for the NASA's hyperspectral Pre-Aerosol-Cloud-Ecosystem (PACE) missions. The results shown here are based on a large collection of satellite imagery, which, along with collections of atmospheric and ocean model data, can be further examined not only to improve HAB detection techniques but also to understand the environmental processes that contribute to such events.

Acknowledgment

The authors would like to thank Dr. S. McCarthy for processing the MODIS monthly composite data, as well as the anonymous reviewers whose multiple comments and suggestions helped to improve this letter significantly. The MODIS data were obtained from NASA (http://ladsweb.nascom.nasa.gov/). This letter is NRL contribution 7330-14-2350.

References

[1] G. M. Hallegraeff, "Manual on Harmful Marine Microalgae," G. M. Hallegraeff, D. M. Anderson, and A. D. Cembella Eds., United Nations Educ., Sci. Cultural Org. (UNESCO), Paris, France, 2003.

[2] P. M. Glibert, D. M. Anderson, P. Gentien, E. Graneli, and K. G. Sellner, "The global, complex phenomena of harmful algal blooms," *Oceanography*, vol. 18, no. 2, pp. 136–147, Jun. 2005.

[3] T. J. Smayda, "Novel and nuisance phytoplankton bloom in the sea: Evidence for global epidemic, in toxic marine phytoplankton," in *Proc. 4th Int. Conf. Toxic Marine Phytoplankton*, E. Graneli *et al.*, Eds., Lund, Sweden, 1990, pp. 29–40.

[4] A. J. McComb, *Eutrophic Shallow Estuaries and Lagoons*. Boca Raton, FL, USA: CRC Press, 1995, p. 240.

[5] J. H. Landsberg, "The effects of harmful algal blooms on aquatic organisms," *Rev. Fisheries Sci.*, vol. 10, no. 2, pp. 113–390, 2002.

[6] A. Sournia, "Red-tide and toxic marine phytoplankton of the world ocean: An inquiry into biodiversity," in *Proc. Harmful Marine Algal Blooms*, P. Lassus *et al.*, Eds., Lavoisier, Paris, 1995, pp. 103–112.

[7] T. J. Smayda, "Harmful algal blooms: Their ecophysiology and general relevance to phytoplankton blooms in the sea," *Limnol. Oceanogr.*, vol. 42, no. 5, pp. 1137–1153, Jul. 1997.

[8] C. V. Hoek, D. G. Mann, and H. M. Jahns, *Algae: An Introduction to Phycology*. Cambridge, U.K.: Cambridge Univ. Press, 1995.

[9] T. J. Smayda, "Turbulence, watermass stratification and harmful algal blooms: An alternative view and frontal zones as pelagic seed banks," in *Proc. Harmful Algae 1*, 2002, pp. 95–112.

[10] J. H. Landsberg and K. A. Steidinger, "A historical review of *Gymnodium breve* red tides implicated in mass mortalities of the manatee (*Trichechus manatus latiriostris*) in Florida, USA," in *Proc. 8th Int. Conf. Harmful Algal Blooms*, B. Reguera, J. Blanco, M. L. Fernandez, and T. Wyatt, Eds., Vigo, Spain, 1998, pp. 97–100.

[11] W. H. Hemmert, "The public health implications of *Gymnodinium breve* red tides: A review of the literature and recent events," in *Proc. 1st Int. Conf. Toxic Dinoflagellate Blooms*, V. R. LoCicero, Eds., 1975, pp. 489–497.

[12] S. Asai *et al.*, "Effects of the toxin of red tide, *Ptychodiscus brevis*, on cannie tracheal smooth muscle: A possible new asthma-triggering mechanism," *J. Allerg. Clinic. Immunol.*, vol. 69, no. 5, pp. 418–428, May 1982.

[13] D. G. Baden, G. Bikhazi, S. J. Decker, F. F. Foldes, and I. Leung, "Neuromuscular blocking action of two brevetoxins from the Florida red tide organism *Ptychodiscus brevis*," *Toxicon*, vol. 22, no. 1, pp. 75–84, 1984.

[14] I. Shulman *et al.*, "Impact of bio-optical data assimilation on short-term coupled physical, bio-optical model predictions," *J. Geophys. Res. Oceans*, vol. 118, no. 4, pp. 2215–2230, Apr. 2013.

[15] R. P. Stumpf *et al.*, "Monitoring *Karenia brevis* blooms in the Gulf of Mexico using satellite ocean color imagery and other data," *Harmful Algae 2*, vol. 2, no. 2, pp. 147–160, Jun. 2003.

[16] J. P. Cannizzaro, K. L. Carder, F. R. Chen, C. A. Heil, and G. A. Vargo, "A novel technique for detection of the toxic dinoflagellate *Karenia brevis* in the Gulf of Mexico from remotely sensed ocean color data," *Continent. Shel. Res.*, vol. 28, no. 1, pp. 137–158, Jan. 2008.

[17] H. R. Gordon *et al.*, "Phytoplankton pigment concentrations in the Middle Atlantic Bight: Comparison of ship determinations and CZCS estimates," *Appl. Opt.*, vol. 22, no. 1, pp. 20–36, 1983.

[18] J. E. O'Reilly *et al.*, "Ocean color chlorophyll a algorithms for SeaWiFS, OC2, and OC4: Version 4," *SeaWiFS Postlaunch Calibration Validation Analyses*, S. B. Hooker and E. R. Firestone, Eds. Greenbelt, MD, USA: NASA Goddard Space Flight Center, 2000, pp. 9–23.

[19] K. L. Carder, F. R. Chen, Z. P. Lee, S. K. Hawes, and D. Kamykowski, "Semi-analytic moderate-resolution imaging spectrometer algorithms for chlorophyll a and absorption with bio-optical domains based on nitrate depletion temperatures," *J. Geophys. Res.*, vol. 104, no. C3, pp. 5403–5421, Mar. 1999.

[20] K. L. Carder *et al.*, "Reflectance model for quantifying chlorophyll-a in the presence of productivity degradation products," *J. Geophys. Res.*, vol. 96, no. C11, pp. 20 599–20 611, Nov. 1991.

[21] D. A. Siegel, S. Maritorena, N. B. Nelson, M. J. Behrenfeld, and C. R. McClain, "Colored dissolved organic matter and its influence on the satellite-based characterization of the ocean biosphere," *Geophys. Res. Lett.*, vol. 32, no. 20, Oct. 2005, Art. ID. L20605.

[22] A. Morel and B. Gentili, "The dissolved yellow substance and the shades of blue in the Mediterranean Sea," *Biogeosciences*, vol. 6, no. 11, pp. 2625–2636, Nov. 2009.

[23] C. A. Brown, Y. Huot, P. J. Werdell, B. Gentili, and H. Claustre, "The origin and global distribution of second order variability in satellite ocean color and its potential applications to algorithm development," *Remote Sens. Environ.*, vol. 112, no. 12, pp. 4186–4203, Dec. 2008.

[24] J. F. R. Gower and G. A. Borstad, "Mapping of phytoplankton by solar-stimulated fluorescence using an imaging spectrometer," *Int. J. Remote Sens.*, vol. 11, no. 2, pp. 313–320, 1990.

[25] R. M. Letelier and M. R. Abbott, "An analysis of chlorophyll fluorescence algorithms for the Moderate Resolution Imaging Spectrometer (MODIS)," *Remote Sens. Environ.*, vol. 58, no. 2, pp. 215–223, Nov. 1996.

[26] M. Babin, A. Morel, and B. Gentili, "Remote sensing of sea surface Sun-induced chlorophyll fluorescence: Consequences of natural variation in the optical characteristics of phytoplankton and the quantum yield of chlorophyll a fluorescence," *Int. J. Remote Sens.*, vol. 17, no. 12, pp. 2417–2448, 1996.

[27] Y. Huot, C. A. Brown, and J. J. Cullen, "New algorithms for MODIS sun-induced chlorophyll fluorescence and a comparison with present data products," *Limnol. Oceanogr. Methods*, vol. 3, pp. 108–130, 2005.

[28] A. Gilerson *et al.*, "Fluorescence contribution to reflectance spectra for a variety of coastal waters," in *Proc. SPIE*, 2007, vol. 6680, pp. 66800C-1–66800C-12.

[29] A. Gilerson *et al.*, "Fluorescence component in the reflectance spectra from coastal waters. Dependence on water composition," *Opt. Exp.*, vol. 15, no. 24, pp. 15 702–15 721, Nov. 2007.

[30] A. Gilerson *et al.*, "Fluorescence component in the reflectance spectra from coastal waters. II. Performance of retrieval algorithms," *Opt. Exp.*, vol. 16, no. 4, pp. 2446–2460, Feb. 2008.

[31] R. Amin *et al.*, "Novel optical techniques for detecting and classifying toxic dinoflagellate *Karenia brevis* blooms using satellite imagery," *Opt. Exp.*, vol. 17, no. 11, pp. 9126–9144, May 2009.

[32] P. Martinolich and T. Scardino, "Automated processing system user's guide version 4.2," Naval Res. Lab. (NRL), Washington, DC, USA, 2011. [Online]. Available: http://www7333.nrlssc.navy.mil/docs/aps_v4.2/html/user/aps_chunk/index.xhtml

[33] R. Amin, "Optical algorithms for assessment of fluorescence sources in sea waters," Ph.D. dissertation, Graduate Center, City Univ. New York, New York, NY, USA, 2009.

[34] R. Amin *et al.*, "Assessing the application of cloud shadow atmospheric correction algorithm on HICO," *IEEE Trans. Geosci. Remote Sens.*, vol. 52, no. 5, pp. 2646–2653, May 2014.

[35] I. M. S. Ramos, "Harmful algal blooms of the West Florida Shelf and Campeche Bank: Visualization and quantification using remote sensing methods," Ph.D. dissertation, Univ. South Florida, Tampa, FL, USA, 2013. [Online]. Available: http://scholarcommons.usf.edu/etd/4775

[36] M. R. Wenand, M. J. W. Veldhuis, and H. J. Woerd, "Estimating phytoplankton biomass in Case II waters using a FLH 2-band algorithm," presented at *Ocean Optics XVIII*, Montreal, QC, Canada, 2006.

[37] C. Hu *et al.*, "Red tide detection and tracing using MODIS fluorescence data: A regional example in SW Florida coastal waters," *Remote Sens. Environ.*, vol. 97, pp. 311–321, 2005.

[38] H. R. Gordon and M. Wang, "Retrieval of water-leaving radiance and aerosol optical thickness over the oceans with SeaWiFS: A preliminary algorithm," *Appl. Opt.*, vol. 33, no. 3, pp. 443–452, 1994.

[39] D. A. Siegel, M. Wang, S. Maritorena, and W. Robinson, "Atmospheric correction of satellite ocean color imagery: The black pixel assumption," *Appl. Opt.*, vol. 39, no. 21, pp. 3582–3591, Jul. 2000.

[40] R. Amin *et al.*, "Impacts of atmospheric corrections on algal bloom detection techniques," presented at the *8th Conf. Coastal Atmos., Ocean. Prediction, Process.*, 2009.

[41] C. Hu, K. L. Carder, and F. E. Muller-Karger, "Atmospheric correction of SeaWiFS imagery over turbid coastal waters: A practical method," *Remote Sens. Environ.*, vol. 74, no. 2, pp. 195–206, Nov. 2000.

[42] M. Wang and W. Shi, "Estimation of ocean contribution at MODIS near infrared wavelengths along the east coast of the U.S.: Two case studies," *Geophys. Res. Lett.*, vol. 32, no. 13, 2005, Art. ID. L13606.

[43] C. Hu, Z. P. Lee, F. E. Muller-Karger, and K. L. Carder, "Application of an optimization algorithm to satellite ocean color imagery: A case study in Southwest Florida coastal waters," in *Proc. SPIE Ocean Remote Sens. Appl.*, J. Frouin, Y. Yuan, and H. Kawamura, Eds., Bellingham, WA, USA, 2003, vol. 4892, pp. 70–79.

[44] C. Hu, F. E. Muller-Karger, and P. W. Swarzenski, "Hurricanes, submarine groundwater discharge, and Florida's red tides," *Geophys. Res. Lett.*, vol. 33, no. 11, Jun. 2006, Art. ID. L11601.

[45] S. Belanger, J. K. Ehn, and M. Babin, "Impact of sea ice on the retrieval of water-leaving reflectance, chlorophyll a concentrations and inherent optical properties from satellite ocean color data," *Remote Sens. Environ.*, vol. 111, no. 1, pp. 51–68, Nov. 2007.

[46] R. Amin, R. W. Gould, W. Hou, Z. P. Lee, and R. Arnone, "Automated detection and removal of cloud shadow on HICO images," in *Proc. SPIE Ocean Sens. Monitoring III*, W. Hou and R. Arnone, Eds., 2011, vol. 8030, pp. 803004-1–803004-10.

[47] R. Amin, R. W. Gould, W. Hou, R. A. Arnone, and Z. P. Lee, "Optical algorithm for cloud shadow detection over water," *IEEE Trans. Geosci. Remote Sens.*, vol. 51, no. 2, pp. 732–741, Feb. 2013.

[48] P. Tester and K. A. Steidinger, "*Gymnodinium breve* red tide blooms: Initiation, transport and consequences of surface circulation," *Limnol. Oceanogr.*, vol. 45, no. 5, pp. 1039–1051, Jul. 1997.